Journal of Physiology (2002), **540.3**, *pp.* 861–873
DOI: 10.1113/jphysiol.2001.013506

www.jphysiol.org

Developmental profiles of glutamate receptors and synaptic transmission at a single synapse in the mouse auditory brainstem

Indu Joshi and Lu-Yang Wang

The Program for Brain and Behavioral Research & Division of Neurology, The Hospital for Sick Children and Department of Physiology, University of Toronto, 555 University Avenue, Toronto, Ontario, Canada M5G 1X8

Using whole-cell recordings from presynaptic terminals and postsynaptic principal neurons in the mouse medial nucleus of the trapezoid body (MNTB), we have characterized properties of the calyx of Held synapse during the first three postnatal weeks. We observed that evoked excitatory postsynaptic currents (EPSCs) mediated by NMDA receptors (NMDAR) increased until postnatal day 11/12 (P11/12) after which they declined to very low or undetectable levels at P16. Meanwhile, EPSCs mediated by AMPA receptors (AMPAR) showed an approximate three-fold increase in amplitude. These changes were paralleled by NMDAR and AMPAR currents evoked by exogenous NMDA and kainate to MNTB neurons except that whole-cell kainate currents remained constant after P7/8 while AMPAR-EPSCs continued to increase. We found that the decay time constant τ for NMDAR-EPSCs and AMPAR-EPSCs declined by about 30 % and 70 %, respectively. Analyses of NMDAR-EPSCs with subunit-specific pharmacological agents including ifenprodil, *N,N,N´,N´*-tetrakis(2-pyridylmethyl)-ethylenediamine (TPEN), zinc and Mg^{2+} revealed subtle developmental changes in subunit composition. As maturation progressed, this synapse displayed a reduction in the number of presynaptic spike failures and the extent of synaptic depression in response to trains of stimuli (50–300 Hz) while the recovery rate from depression accelerated. These results demonstrate profound changes in the size and kinetics of postsynaptic glutamate receptors and in the spike-firing capability of presynaptic terminals at the calyx of Held–MNTB synapse during early development. We suggest that these concurrent presynaptic and postsynaptic adaptations represent important steps for synapse consolidation and refinement and ultimately for the development of fast high-fidelity transmission at this synapse.

(Resubmitted 5 November 2001; accepted after revision 8 February 2002)
Corresponding author L.-Y. Wang: Division of Neurology, The Hospital for Sick Children, 555 University Avenue, Toronto, Ontario, Canada M5G 1X8. Email: luyang.wang@utoronto.ca

Synaptic strength can be modified by different patterns of input activity, leading to different forms of short- and long-term synaptic plasticity (Zucker, 1989; Bliss & Collingridge, 1993; Malenka, 1994). Immature synapses in developing brains exhibit robust plasticity (Crair & Malenka, 1995; Kirkwood *et al.* 1995; Izumi & Zorumski, 1995). Because of the small size of typical central synapses and the complexity of polysynaptic innervation, it is difficult to determine whether such plasticity is due to changes in presynaptic quantal output or postsynaptic responses. To gain insights into developmental plasticity in central synapses, we have employed the glutamatergic calyx of Held synapse located in the mouse medial nucleus of the trapezoid body (MNTB) as a model system. This model presents several advantages. First, since each MNTB neuron receives a single calyx input at the soma, we can investigate synaptic properties at the single synapse level. Second, because adequate voltage-clamping of the membrane potential can be attained at the soma, the shape and size of the recorded excitatory postsynaptic currents (EPSCs) mediated by NMDA and AMPA receptors (NMDARs and AMPARs) can be reliably used to analyse the amount of transmitter release as well as the kinetics and density of postsynaptic receptors. Finally, the compact axosomatic structure and the accessibility of nerve terminals to electrodes allows for the uncoupling of presynaptic and postsynaptic mechanisms.

The calyx of Held–MNTB synapse is an important relay station capable of phase-locking its activity to high input rates, and is thus thought to be critical for the preservation of timing information used in sound localization (Trussell, 1999). Although there are detailed accounts of the morphological changes in this synapse at various postnatal stages (Morest, 1968; Kuwabara *et al.* 1991), much less is known about the functional development of high-fidelity synaptic transmission particularly in mice (Futai *et al.* 2001). We have characterized developmental changes in

synaptic properties of the mouse calyx of Held–MNTB synapse within the first three postnatal weeks. We found that synaptic NMDARs were present only transiently within the first 2 weeks, and exhibited a unique developmental profile. Although synaptic AMPARs exhibited a nearly linear growth in density over the same period, the total population of functional AMPARs (i.e. whole-cell kainate currents) reached a maximum by the end of the first postnatal week. We suggest that these changes, along with concurrent alterations in kinetic properties of EPSCs and in synaptic depression and recovery, contribute significantly to the development of high-fidelity synaptic transmission at this synapse. Part of this study had been previously published in abstract form (Joshi & Wang, 2000).

METHODS

Slice preparation

Mice were housed in the facility certified by the Canadian Council of Animal Care and used for this study according to a protocol approved by the Hospital for Sick Children Animal Care Committee. Brainstem slices were prepared from P3–P18 mice (CD1/C57 black) as previously described (Forsythe & Barnes-Davis, 1993). Mice were decapitated with a small guillotine and brains were rapidly dissected and immersed in ice-cold artificial CSF (aCSF) containing (mM): NaCl 125, KCl 2.5, glucose 10, NaH_2PO_4 1.25, Na-pyruvate 2, myo-inositol 3, ascorbic acid 0.5, $NaHCO_3$ 26, $MgCl_2$ 1, and $CaCl_2$ 2, at a pH of 7.3 when bubbled in 95 % O_2 and 5 % CO_2. Transverse slices of the auditory brainstem were cut at a thickness of 225–300 μm using a vibratome (Leica VT100S) and incubated at 37 °C for 1 h and thereafter kept at room temperature for experiments (20–22 °C).

Electrophysiology

Whole-cell patch-clamp recordings were made from visually identifiable postsynaptic MNTB neurons or presynaptic calyces with an Axopatch 200B amplifier (Axon Instruments). For postsynaptic voltage-clamp recordings, the patch electrodes had a resistance of 2–4 MΩ and were filled with intracellular solution containing (mM): potassium gluconate 97.5, CsCl 32.5, EGTA 5, Hepes 10, $MgCl_2$ 1, TEA 30 and lidocaine *N*-ethyl bromide (QX314) 3, pH 7.2. The same solution was used to fill electrodes (4–6 MΩ) for presynaptic current-clamp recordings except that CsCl was replaced by KCl. To block inhibitory inputs, bicuculline (10 μM) and strychnine (1 μM) were added to the aCSF. EPSCs or presynaptic spikes were evoked by stimulating the presynaptic axon fibre bundles with a bipolar platinum electrode placed near the midline of the slice. Stimulation voltage was set at 20–30 % above the threshold. Series resistance for postsynaptic recordings was 4–8 MΩ and compensated to 90 % with a lag of 10 μs. Data were filtered at 2 kHz, digitized at 10–20 kHz, acquired online, and analysed off-line with pCLAMP7 software (Axon Instruments). Current density (nA pF^{-1}) was estimated by normalizing the peak amplitudes of EPSCs to the capacitance of the recorded cell. Averaged data are expressed as mean ± standard error of the mean (S.E.M.). For pharmacological experiments, drugs were mixed into aCSF and focally applied to the recorded cells using a square glass pipette (400 μm in width) placed on the surface of the slice. The jet solution had a linear range of 1–2 mm and completely replaced the solution surrounding the recording region within 30–60 s. Bicuculline, strychnine, kainate, NMDA, $ZnCl_2$, *N,N,N′N′*-tetrakis(2-pyridylmethyl)-ethylenediamine (TPEN) and glycine, were obtained from Sigma and QX314 and ifenprodil were from Tocris.

RESULTS

Characterization of developmental changes in EPSCs mediated by NMDARs and AMPARs

We first investigated age-dependent changes in synaptic responses by making whole-cell voltage-clamp recordings from MNTB neurons in slices taken from mice ranging from 5 to 18 days old. When the presynaptic axon bundle was stimulated, the calyx of Held–MNTB synapse typically exhibited very large all-or-none responses as previously shown (Forsythe & Barnes-Davies, 1993; Wang, 2000). Evoked EPSCs consisted of a fast AMPA component (AMPAR-EPSC) and a slow NMDA component (NMDAR-EPSC). Figure 1*A* shows three recordings of evoked EPSCs recorded from P5, P9 and P14 synapses at various holding potentials, from which we constructed normalized current (*I*)–voltage (*V*) curves (Fig. 1*B* and *C*). The *I–V* curves for AMPAR-EPSCs are linear and their slopes increase in an age-dependent manner, indicating an increase in synaptic conductance (Fig. 1*B*). On the other hand, NMDAR-EPSCs of all ages display the typical rectification at negative potentials due to Mg^{2+} block. The amplitude of NMDAR-EPSCs at positive potentials increases by approximately two-fold at P9 compared to that at P5, but at P14 it declines to a level even lower than that at P5. As the synapse matures, there is a significant change in the ratio between NMDAR- and AMPAR-EPSCs at the same holding potential (i.e. 0.62 at P5 *vs.* 0.89 at P9; +60 mV). The results of different age groups are summarized in Fig. 1*D* and *E* in which the peak current density (at +60 mV) of AMPAR- and NMDAR-EPSCs, recorded from the same synapses, are plotted. The current density of AMPAR-EPSCs is relatively lower than that of NMDAR-EPSCs at P5/6, but rapidly increases by more than three-fold over the first two postnatal weeks (Fig. 1*D* and *E*). This overall developmental profile of AMPAR-EPSC appears to be consistent with some studies at the calyx-type synapse (Bellingham *et al.*1998; Chuhma & Ohmori, 1998; but see Taschenberger & von Gersdorff, 2000; Iwasaki & Takahashi, 2001, and Discussion). The developmental changes in NMDAR-EPSCs, however, differ from the aforementioned two studies (Bellingham *et al.*1998; Chuhma & Ohmori, 1998) but are consistent with a recent study carried out in mice (Futai *et al.* 2001). We observed an initial increase in NMDAR-EPSCs up to the age when sensory input begins (i.e. P11/12). We have previously shown that synaptic NMDARs are not saturated by a single stimulus (Wang, 2000) and subsynaptic reorganization of NMDARs in developing synapses may alter their responsiveness. We therefore applied a train of stimuli (100 Hz, 100 ms) to recruit and assay a larger population of synaptic NMDARs (Fig. 2*A–C*). Again, we

found a sharp reduction in the peak amplitude of accumulative responses after P11/12. Most surprisingly, the prominent NMDAR-EPSCs in immature synapses were almost absent in mature synapses (e.g. P16) (Fig. 2*C* and *D*). This is a rather unique observation since NMDARs and AMPARs are usually co-localized in most central synapses. The marked decrease in the size of the NMDAR-EPSCs beyond maturation raises the possibility that

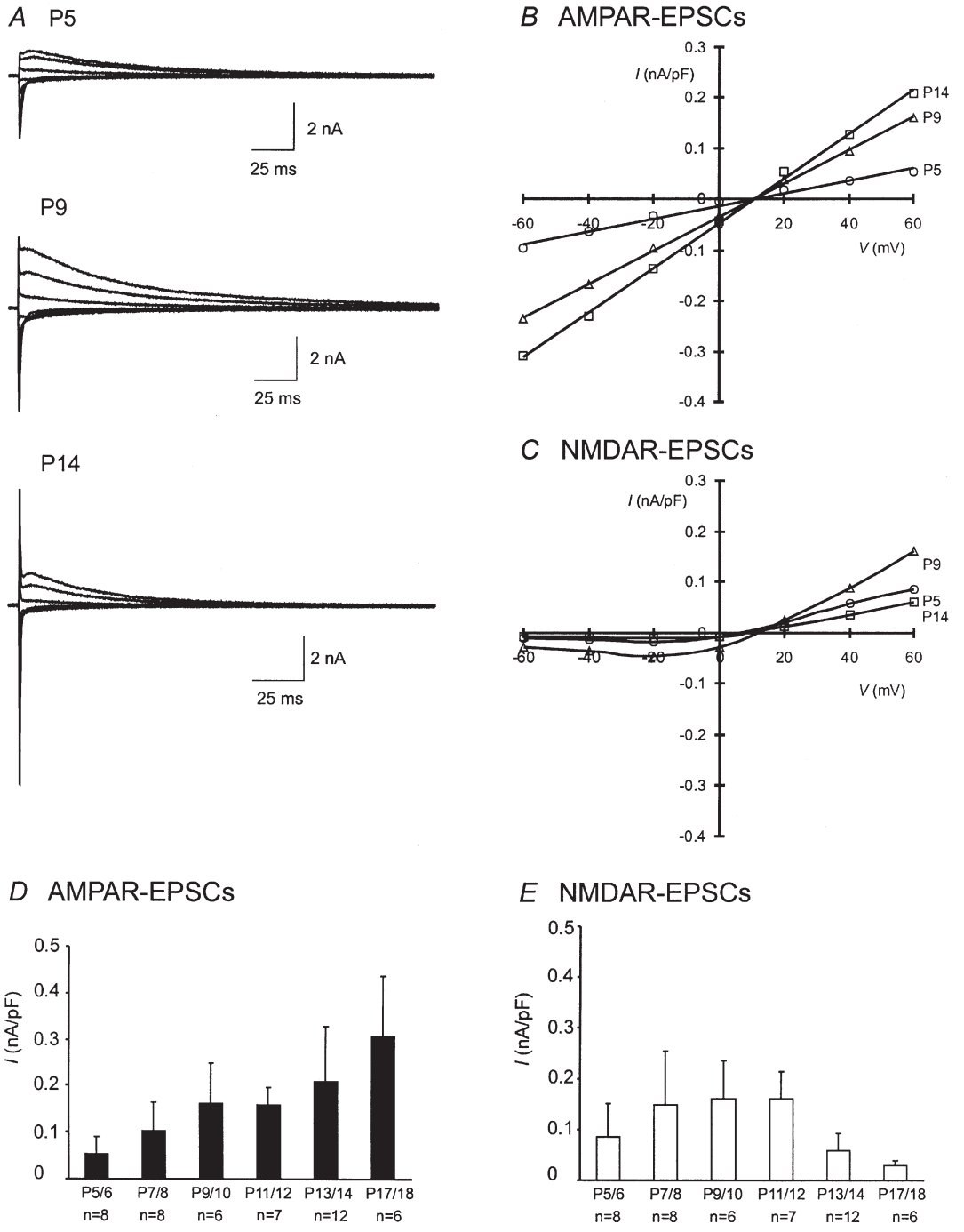

Figure 1. Developmental changes in the amplitude of AMPAR- and NMDAR-EPSCs

A, examples of EPSCs recorded from P5, P9 and P14 synapses are shown. Current traces at different holding potentials ranging from −60 to +60 mV in 20 mV increments are superimposed for each synapse. *B* and *C*, the peak amplitude of AMPAR- and NMDAR-EPSCs in *A* at various holding potentials for each synapse is normalized to its capacitance, and plotted for current (*I*)–voltage (*V*) relationships. *D* and *E*, the current densities at (+60 mV) in *B* and *C* for both AMPAR- and NMDAR-EPSCs of each age group are pooled and plotted. The data are presented as means ± S.E.M. and *n* indicates the number of cells in each age group in this and subsequent figures.

NMDARs are particularly critical for the early formation and consolidation of the calyx of Held–MNTB synapses.

Developmental profiles of total NMDARs and AMPARs in MNTB neurons

Because MNTB neurons are compact without extensive processes and largely encompassed by the calyx terminal, we reason that glutamate receptors are primarily expressed on the soma. The total population of functional NMDARs and AMPARs (synaptic and extrasynaptic receptors) in developing neurons can thus be assessed by applying exogenous agonists. We activated NMDARs and AMPARs by applying NMDA (0.3 mM + glycine 10 μM) and kainate (0.3 mM) using a fast local perfusion pipette, which reduces receptor desensitization associated with the relatively slow solution exchange rate in slices (see Methods). Voltage ramps (−60 to +60 mV, 100 ms) in the absence and presence of each agonist were used to measure the net currents mediated by NMDARs and AMPARs in the same cell. We surveyed whole-cell responses in MNTB neurons starting at P3. Panels *A* and *B* in Fig. 3 contrast two such recordings from MNTB neurons at P3 and P12. We observed a reversal of the ratio of kainate to NMDA currents in these experiments (from 0.72 at P3 to 2.2 at P12). Figure 3*C* summarizes the age-dependent changes in the steady-state current density at +60 mV. The developmental profile of NMDAR-mediated currents well parallels that of synaptic NMDAR-EPSCs (Figs 1*E* and 2*D*). However, different from a nearly linear increase in synaptic AMPAR-EPSCs over the same time frame (Fig. 1*D*), whole-cell kainate-evoked currents initially increased but reached a plateau level after P7/8. Because kainate can partially desensitize AMPA receptors, we repeated this set experiments in two age groups (i.e. P7/8 and P11/12) after application of cyclothiazide (CTZ, 100 μM), which blocks desensitization of AMPARs (Yamada & Rothman, 1992; Patneau *et al.* 1993; Trussel *et al.* 1993). We found that the current density slightly increased when compared to that measured in the absence of CTZ at the same developmental stages (P7/8, control 0.56 ± 0.23 nA pF^{-1} *vs.* CTZ 0.62 ± 0.15 nA pF^{-1}, $P > 0.05$; P11/12, control 0.47 ± 0.16 nA pF^{-1} *vs.* CTZ 0.68 ± 0.07 nA pF^{-1}, $P > 0.05$, Student's paired *t* test), indicating that the kainate currents we recorded reliably reflected the activity of AMPARs on MNTB neurons. Since kainate presumably activates both synaptic and extrasynaptic receptors, the divergent developmental

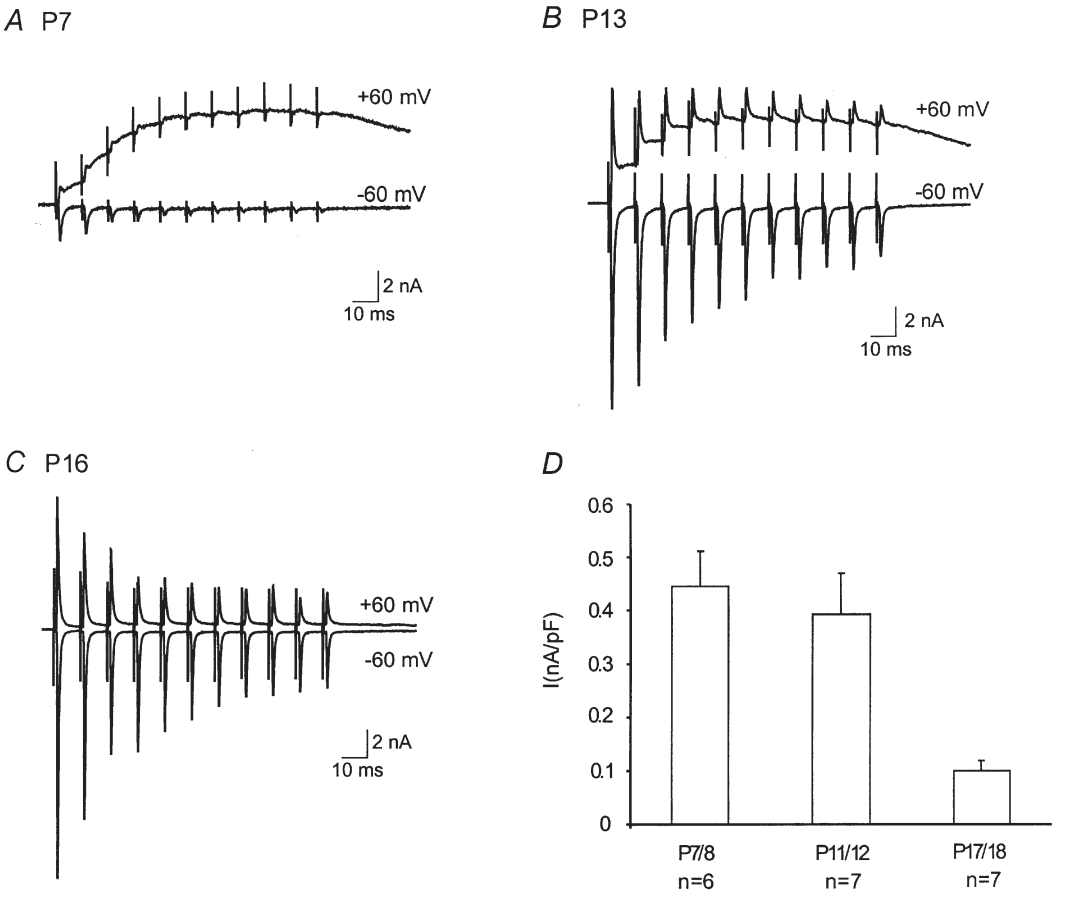

Figure 2. Maturing synapses display a decrease in synaptic NMDARs

A, *B* and *C*, comparison of EPSCs from P7, P13 and P16 synapses during 100 Hz stimulation trains (100 ms) at +60 and −60 mV. Note the absence of build-up of NMDAR-EPSCs at +60 mV at the P16 synapse. *D*, plot of pooled current densities at +60 mV for the each age group.

profiles of whole-cell kainate currents and AMPAR-EPSCs suggest that there may be significant reorganization of synaptic and extrasynaptic AMPARs leading to an enhancement in synaptic strength.

Acceleration in the decay kinetics of synaptic NMDAR- and AMPAR-EPSCs

We next analysed the kinetic properties of AMPAR- and NMDAR-EPSCs. Panels *A* and *B* in Fig. 4 compare the decay time course of these EPSCs from synapses at P5 and P13. After normalization of the peak amplitude for each component, we observed a clear acceleration in the decay kinetics for both the AMPAR- and NMDAR-EPSCs in more mature synapses. When the falling phase of the AMPAR-EPSC (at −60 mV) was fitted with a single exponential function, we found that the time constants decreased by about 70 % from P5 to P13 (Fig. 4*A*). Similarly, the decay time constants for the NMDAR-EPSC (at +60 mV) also decreased, though less prominently than those of AMPAR-EPSCs (Fig. 4*B*). Figure 4*C* and *D* summarize the changes in the kinetics of NMDAR- and AMPAR-EPSCs for all ages. Our observation of synaptic AMPAR decay kinetics is consistent with some previous studies (Taschenberger & von Gersdorff, 2000; Futai *et al.* 2001; Iwasaki & Takahashi, 2001), although conflicting observations have been reported (Chuhma & Ohmori, 1998).

Subunit composition of synaptic NMDARs

Given the unique developmental features of NMDAR-EPSCs and changes in their decay kinetics, we further investigated the changes in the subunit composition of synaptic NMDARs. Since the decay kinetics of NMDAR-EPSCs is usually dictated by channel gating kinetics of NMDARs (Clements, 1996), it is conceivable that the accelerated decay of NMDAR-EPSCs is a result of a subunit switch in the composition of synaptic NMDARs during development. For example, subunit switching from the slow-gating NR2B to the fast-gating NR2A subunit has been seen at other central synapses (Takahashi *et al.* 1996; Stocca & Vicini, 1998; Tovar & Westbrook, 1999). To test this idea, we examined several reagents that are known to interact with NMDARs in a subunit-specific manner. Figure 5*A*–*C* compares typical recordings from P6 and P12 synapses in response to ifenprodil, which selectively blocks NMDARs dominated by the NR2B subunit (Williams, 1993; Tovar & Westbrook, 1999), and to Zn^{2+} (100 nM) and (TPEN), two reagents that specifically target NMDARs containing NR2A subunits (Paoletti *et al.* 1997; Xiong *et al.* 1999). We found that ifenprodil (5 μM) produced a marginal inhibition of NMDAR-EPSCs (< 25 %) and that this inhibition seemed to increase slightly over the first two postnatal weeks, suggesting that there is a slight increase in the expression of NR2B. A low concentration of Zn^{2+} (100 nM), which can effectively block NR2A-enriched NMDARs, produced a slight inhibition of NMDAR-EPSCs (< 10 %). In contrast, TPEN (5 μM), which is known to remove endogenous Zn^{2+}, led to a limited potentiation of NMDAR-EPSCs (~5 %). Neither the inhibition by Zn^{2+} nor the potentiation by TPEN showed any age dependence (Fig. 5*D*). Collectively, the last three lines of evidence indicate that both NR2A and NR2B subunits are likely present throughout various developmental stages, but subunit

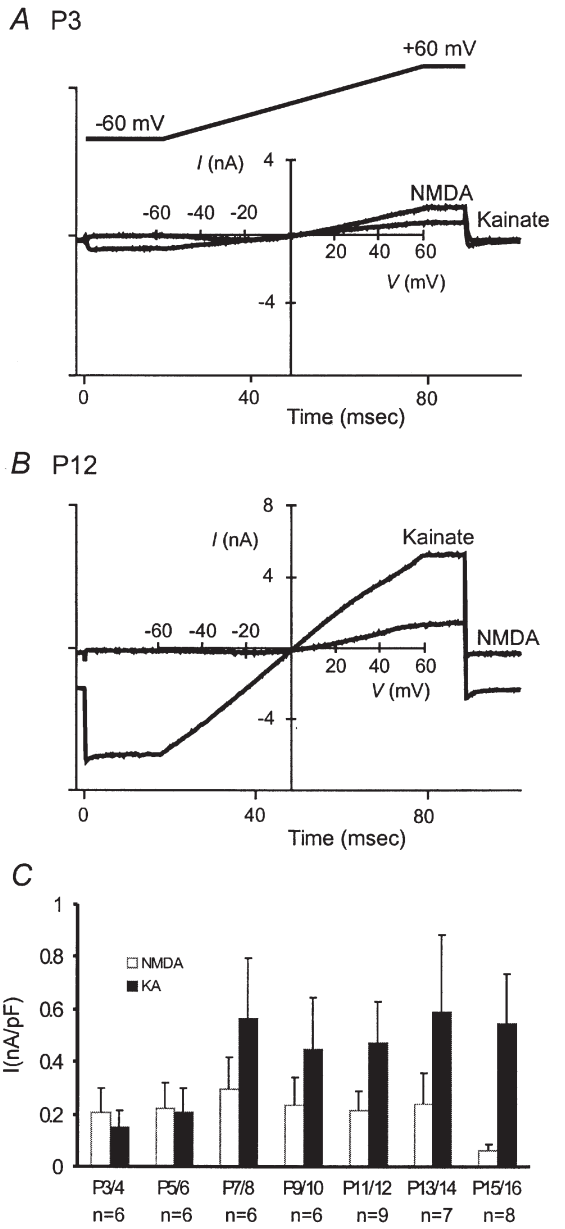

Figure 3. Age-dependent changes in total currents evoked by exogenously applied agonists

A and *B*, whole-cell current responses following the application of exogenous NMDA (0.3 mM) and kainate (0.3 mM) to P3 and P12 MNTB neurons. NMDA (+10 μM glycine) and kainate were applied to the same cell in separate trials. The holding potential was −20 mV and the leak currents were determined from voltage ramps (−60 to +60 mV, 100 ms; inset in *A*) in control solution prior to each agonist application and subtracted. *C*, a plot of whole-cell current density at +60 mV for different age groups.

switching between these two subunits is an unlikely mechanism underlying the accelerated decay of NMDAR-EPSCs (see Discussion). Finally, we used Mg^{2+} (50 μM) as a probe for NMDARs containing NR2C and NR2D, which usually have a lower sensitivity to voltage-dependent blockade by this divalent ion. Figure 5*E* shows two recordings of NMDAR-EPSCs at a holding potential of −60 mV from a P6 and P12 synapse in the presence and absence of Mg^{2+} (50 μM). It is apparent that Mg^{2+} blocked a greater portion of the current in the P12 synapse than in the P6 synapse. A significant increase in the extent of block at P11/12 (Fig. 5*F*) suggests a transient reduction in NR2C and NR2D subunits. Because NMDARs containing NR2C/2D usually have slower gating kinetics than those containing NR2A/2B, the transient reduction in NR2C/2D may contribute to the decrease in the decay time constant seen at the same age (P11/12). In light of these observations and those in the literature describing pharmacological phenotypes of NMDARs with different subunit combinations (McBain & Mayer, 1994; Cull-Candy *et al.* 2001), we suggest that there are perhaps only subtle changes in the subunit composition of synaptic NMDARs during development of the calyx of the Held–MNTB synapse.

Fidelity of high-frequency synaptic transmission

The calyx of the Held–MNTB synapse is specialized to preserve the fidelity of high-frequency synaptic transmission. To examine the behaviour of this synapse under physiological conditions, we recorded AMPAR-EPSCs in response to trains of high-frequency stimuli (50–300 Hz, 100 ms). We found that all synapses were capable of responding to frequencies below 100 Hz, but multiple failures were noted in young synapses at higher frequencies. Figure 6*A–C* shows recordings from three synapses (P5, P9 and P14) when stimulated at 200 Hz. We observed that P5 and P9 synapses exhibited more profound synaptic depression and failures (indicated by arrows) than P14 synapses. The number of failures from different age groups are plotted in Fig. 6*D*, which clearly shows a significant age-dependent decrease. These failures appeared to be independent of extracellular Ca^{2+} concentration as a reduction of Ca^{2+} from 2 to 1 mM did not significantly change the number of failures in immature synapses

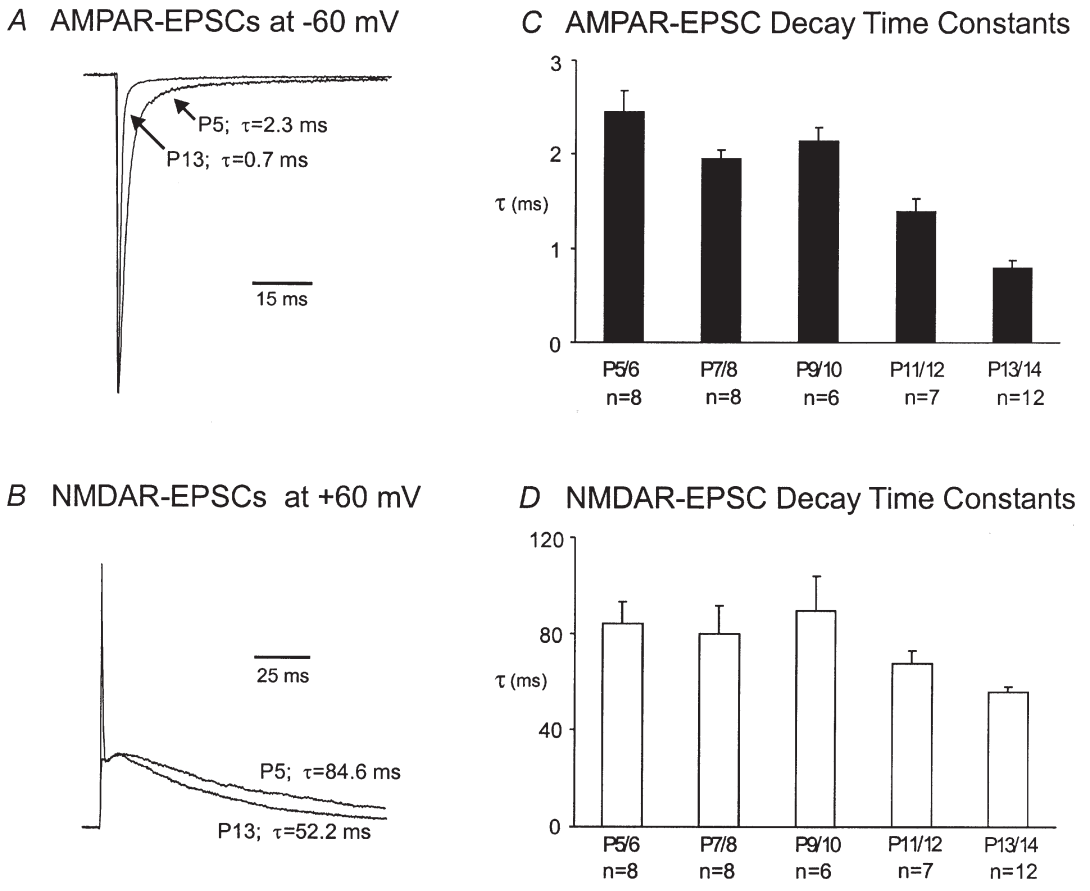

Figure 4. Acceleration in the decay kinetics of AMPAR- and NMDAR-EPSCs

A and *B*, current traces recorded from P5 and P13 synapses are normalized and superimposed for comparison of the decay time course for AMPAR- and NMDAR-EPSCs. Note that only the *x*-axis calibration bars are given due to normalization. Decay time constants (τ, ms) obtained by fitting the falling phase of EPSCs with single exponential function are given. *C* and *D*, plots of pooled for AMPAR- and NMDAR-EPSCs for each age group.

(Fig. 6*E*). If these failures were due to a depletion of presynaptic vesicles or desensitization of postsynaptic receptors, one would expect a reduction in initial quantal output by lowering extracellular Ca^{2+} to decrease the number of failures. These observations suggest that other presynaptic mechanisms may be responsible for these failures. To further investigate the nature of synaptic failures, we directly recorded firing patterns from presynaptic calyces in response to various test frequencies. Figures 6*F* and *G* contrast two current-clamp recordings of presynaptic spikes from P7 and P15 synapses. At 100 Hz, both calyces were capable of generating spikes when presynaptic axons were stimulated (top panels). In contrast, the P7 calyx failed to follow stimulation inputs at 200 Hz while the P15 calyx responded with high fidelity (bottom panels). It should be noted that the pattern of presynaptic spike failures resembles those of EPSCs at this frequency (Fig. 6*A* and *B*), indicating that the inability of immature terminals to fire at high frequencies likely accounts for the Ca^{2+}-independent failures at this synapse.

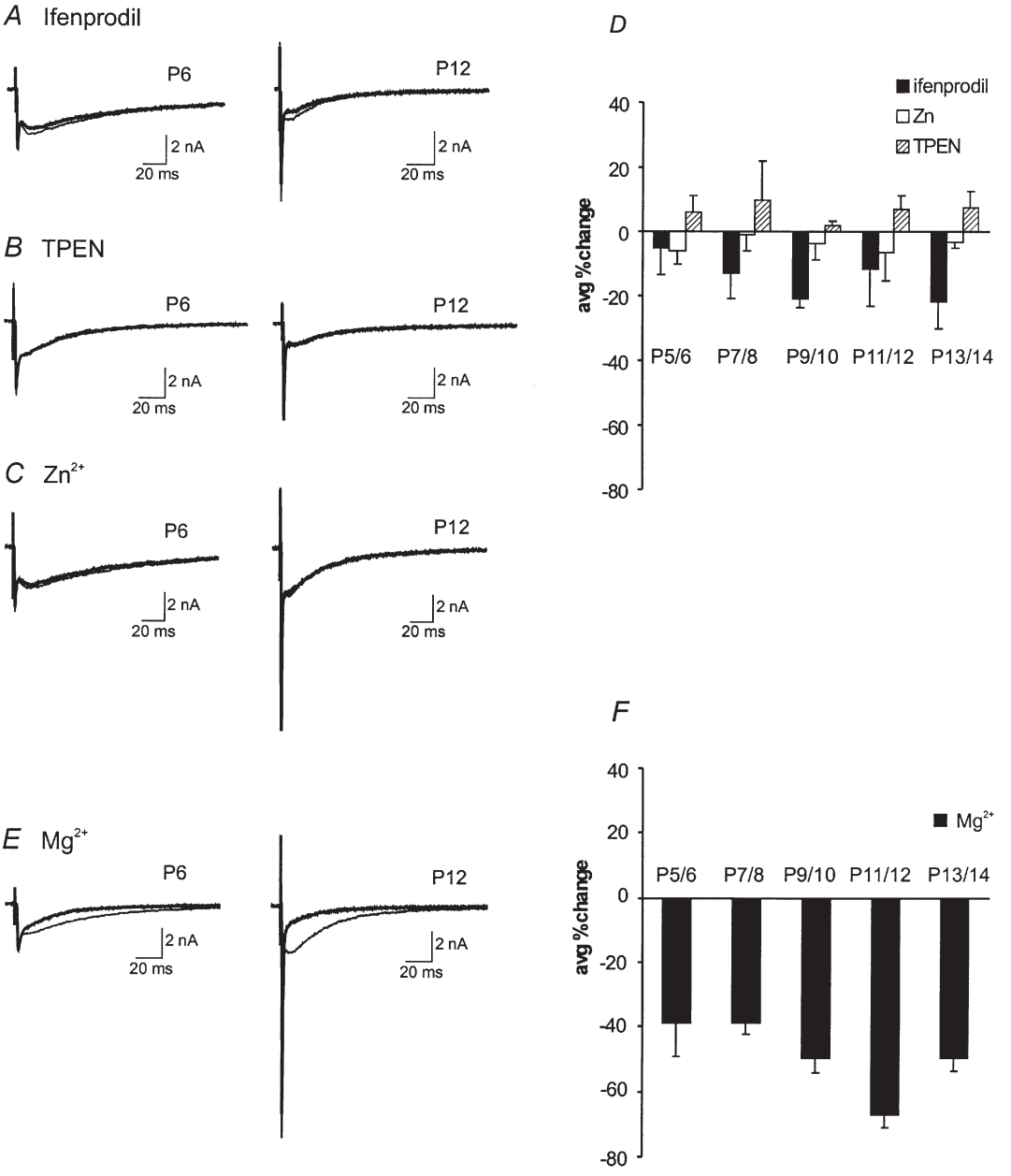

Figure 5. Developmental changes in NMDAR subunits

Current traces before and after exogenous application of NMDAR subunit-specific reagents: *A*, ifenprodil (5 μM); *B*, TPEN (5 μM); *C*, Zn^{2+} (100 nM) at P6 and P12. *D*, a summary plot of the average percentage change from control after application of these agents for different age groups ($n = 5$ for each group). *E*, current traces before and after the application of Mg^{2+} (50 μM) at P6 and P12. *F*, the average percentage change of block after Mg^{2+} application is plotted for all ages ($n = 5$ for each group). The thinner traces represent controls while thicker traces represent applied reagents in *A*–*C* and *E*.

Synaptic depression and recovery in developing synapses

When presynaptic axons were stimulated at high frequencies, AMPAR-EPSCs showed robust short-term synaptic depression (Figs 6 and 7). This depression exhibits strong age dependence. For example, the ratio of the last to first EPSC in response to 100 ms train at 100 Hz increased by nearly four-fold from P7/8 to P17 (Fig. 7*A–D*). Among many possible factors responsible for synaptic depression, depletion of presynaptic vesicles and desensitization of

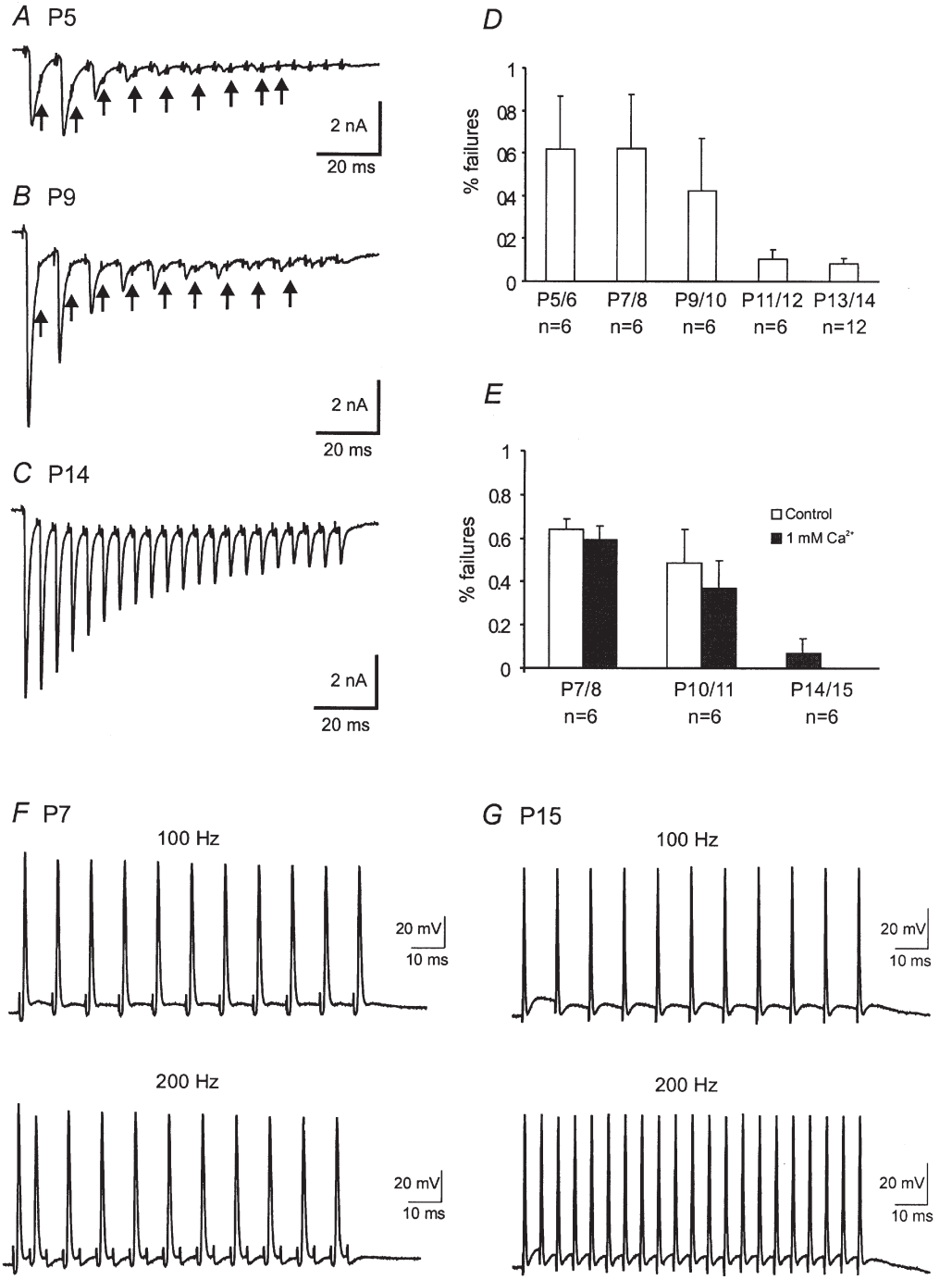

Figure 6. Developmental changes in synaptic failures, depression and presynaptic action potentials

A–C, AMPAR-EPSCs recorded in response to a train of stimuli (100 ms, 200 Hz) from three synapses, P5, P9 and P14, respectively. Note that there was a significant reduction in the extent of synaptic depression and failures as indicated by arrows. *D*, a plot of the number of failures (200 Hz) for different age groups. *E*, comparison of the number of failures (200 Hz) in 2 and 1 mM Ca^{2+} for different age groups. *F* and *G*, presynaptic spikes recorded at 100 and 200 Hz from a P7 and P15 synapse respectively. Small deflections near the baseline preceding spikes or failures are stimulation artifacts.

postsynaptic receptors represent two primary underlying mechanisms. It has been previously shown that synaptic depression at this synapse can be largely accounted for by a depletion of the readily released pool (RRP) of synaptic vesicles (von Gersodorff *et al.* 1997; Wang & Kaczmarek, 1998). It is also independent of presynaptic inactivation of Ca^{2+} currents and desensitization of postsynaptic receptors in P12–15 mice (Wang & Kaczmarek, 1998). To further explore the role of desensitization in synaptic transmission in immature synapses, we compared the extent of depression

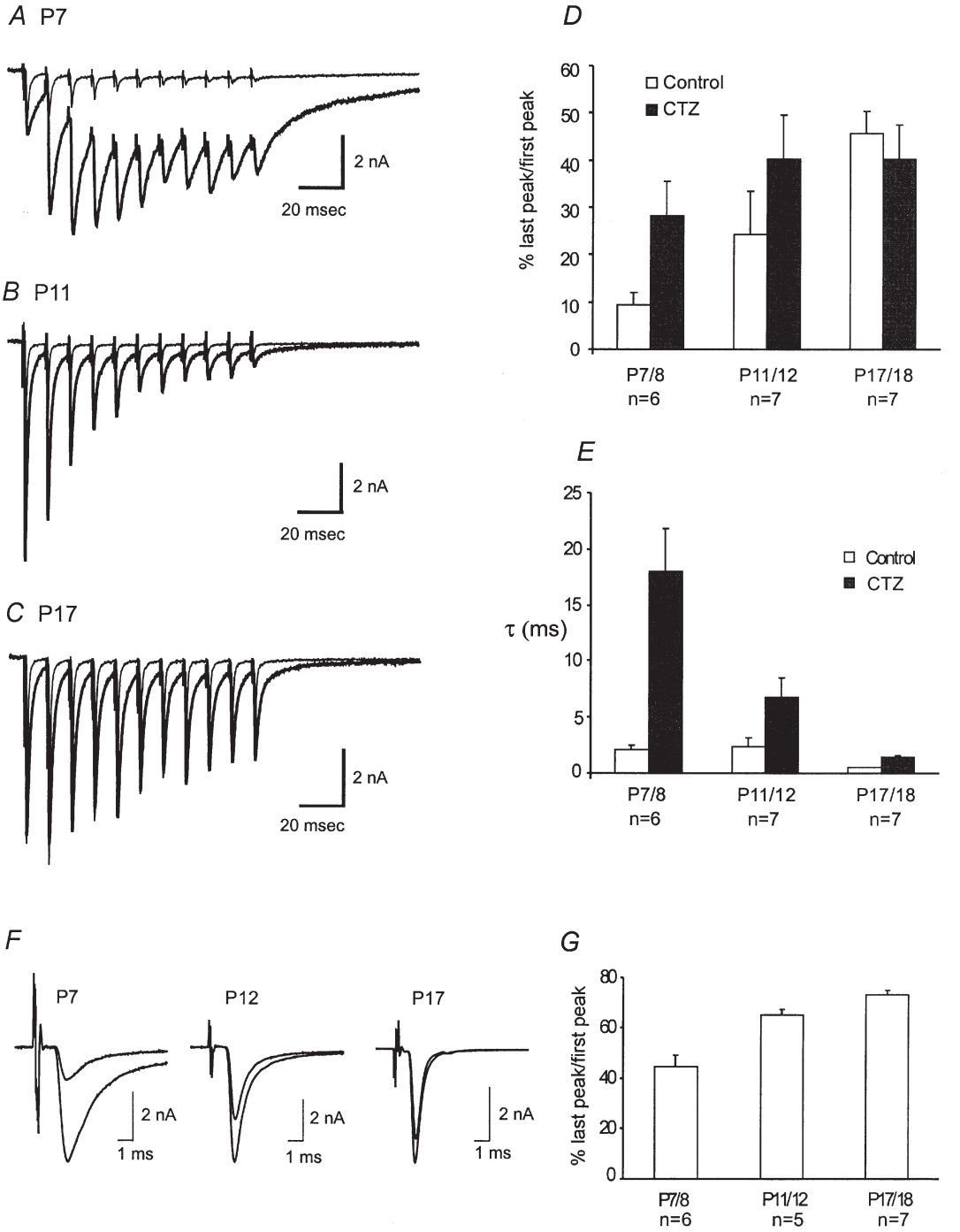

Figure 7. The role of desensitization in synaptic depression

A–C, superimposed traces of AMPAR-EPSCs recorded in response to train stimuli (100 ms, 100 Hz) before and after application of CTZ at P7, P11 and P17, respectively. Thinner traces represent control while thicker traces indicate responses after CTZ application. *D*, pooled data compare the ratio of the last peak to the first peak in control and CTZ for different age groups. *E*, a plot of the decay time constants (τ, ms) for both control and CTZ at varying age groups. *F*, current traces in response to low-frequency trains (10 s, 1 Hz) for P7, P12, and P17. The last EPSC is superimposed over the first EPSC for comparison. *G*, pooled data of the ratio of last peak to first peak from *F* are plotted for different age groups.

in the absence and presence of CTZ (Fig. 7*A–D*). Application of CTZ (100 μM) slowed decay kinetics of AMPR-EPSCs and increased the ratio of the last to first EPSC (Fig. 7*A–C* and *E*). Both effects were particularly pronounced in the P7/8 group. These observations suggest that desensitization likely contributes to the short-term depression in young synapses but not in mature synapses (i.e. P17/18). However, it should be emphasized that CTZ has been shown to increase glutamate release by directly blocking presynaptic K^+ channels at this synapse in juvenile rats (Ishikawa & Takahashi, 2001). The CTZ-induced increase in the ratio of the last to first EPSC in P7/8 is likely confounded by direct presynaptic actions of CTZ. In fact, the ratio of the last EPSC to the second EPSC, which is the largest event in the train, only increased marginally in the presence of CTZ (i.e. Fig. 7*A*). Knowing the presynaptic actions of CTZ, we adapted a different stimulation protocol to test the role of desensitization in synaptic depression without using this reagent. We applied the same number of stimuli as in short trains but at a low frequency of 1 Hz and compared the ratio of the last to first EPSC (Fig. 7*F* and *G*). We found that this protocol led to a greater increase in the ratio of the P7/8 group than the other two groups, when compared to the short high-frequency train protocol (Fig. 7*G vs. D*). Our interpretation of these observations is that much longer inter-pulse intervals at 1 Hz may have reduced accumulative desensitization associated with high-frequency stimulation. We suggest that both desensitization and depletion of the RRP contribute to pronounced depression in young synapses (e.g. P7/8) but depletion is likely the main mechanism underlying synaptic depression in more mature synapses.

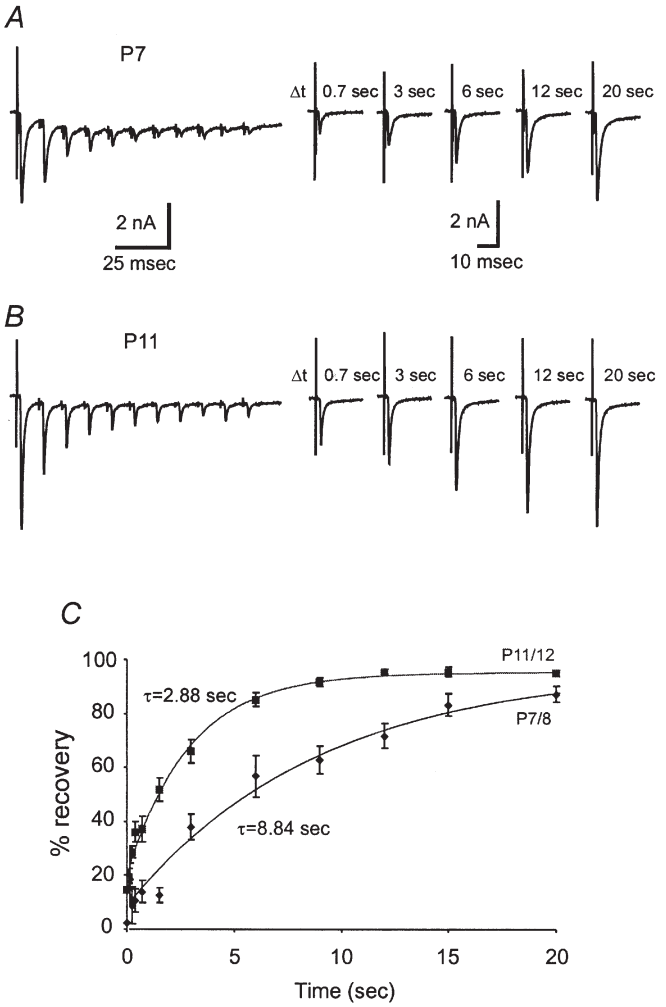

Figure 8. Developmental changes in recovery from synaptic depression

A and *B*, two recordings are shown for comparison of recovery kinetics of P7 and P11 synapses. Recovery from synaptic depression was measured by delivering a single test pulse at different intervals (Δt) following a train of stimuli (100 ms, 100 Hz). Note that no failures were observed at this stimulation frequency. *C*, the ratio of the test pulse EPSC to the first EPSC of the train was used to measure the percentage of recovery. Pooled data for two age groups, P7/8 and P11/12 ($n = 7$ for each group), are fitted with a single exponential function and time constants are given.

To provide insights into developmental changes in the kinetics of replenishment of the RRP and removal of desensitization, we next examined recovery from synaptic depression. In order to measure the recovery from synaptic depression of synapses in different age groups, we first delivered a train of stimuli at 100 Hz (100 ms), a frequency at which all synapses were able to follow without failures (Fig. 6*F* and *G*), and then administered a test pulse at different time intervals following the train. Figure 8*A* and *B* shows two typical recordings from P7 and P11 synapse. We found that the P11 synapse recovered faster than the P7 synapse even though both synapses were equally depressed at the end of the test train. The pooled results for P7/8 and P11/12 age groups are depicted in Fig. 8*C*, in which the time course for recovery was well described by a single exponential function. The time constants derived from fittings reveal an approximate three-fold increase in the recovery rate, being about 9 s at P7/8 and 3 s at P11/12. The latter value falls in a similar range as previously reported for the same age group (von Gersodorff *et al.*1997; Wang & Kaczmarek, 1998). These results demonstrate that recovery from short-term depression is accelerated during development of this synapse.

DISCUSSION

We have characterized developmental changes in synaptic properties in the mouse calyx of the Held–MNTB synapse within the first three postnatal weeks. This is a critical period during which synapse formation at P4/5, sensory onset at P11/12, and morphological maturation after P14 take place (Morest, 1968; Kuwabara *et al.* 1991). We found a significant age dependence in the size and kinetics of EPSCs as well as in the synaptic fidelity, depression and recovery dynamics from depression. Many studies have

addressed similar issues in other central synapses (Carmignoto & Vicini, 1992; Hestrin, 1992; Takahashi *et al.* 1996; Flint *et al.* 1997), but it is difficult to compare our observations made at the single synapse level with those based on complex synaptic connections. Our results are partially consistent with previous reports studying developmental plasticity of the calyx-type synapse in rat (Bellingham *et al.* 1998; Chuhma & Ohmori, 1998; Taschenberger & von Gersdorff, 2000; Iwasaki & Takahashi, 2001).

Similar to what we have described, it has been reported that AMPAR-EPSCs show an age-dependent increase in amplitude at both the rat calyx of Held (Chuhma & Ohmori, 1998) and the endbulb of the Held synapse (Bellingham *et al.* 1998). The former study attributed this increase to an upregulation of presynaptic voltage-gated Ca^{2+} channels and release probability, whereas the latter suggested a postsynaptic increase in synaptic conductance. Independent of presynaptic changes, we have shown that exogenous kainate used to activate AMPARs produced an approximate three-fold increase in the current density after P7/8, suggesting a direct increase in the density of functional AMPARs or alternatively a subunit gating switch from small to large conductance channels (e.g. a decrease in the relative proportion of GluR2). It is interesting to note that the whole-cell kainate current, which represents an activation of both synaptic and extrasynaptic receptors, appeared to have reached a plateau by P7/8 (Fig. 3*C*), whereas the synaptic AMPAR-EPSCs continued to increase over the following week. An increase in the clustering of existing AMPARs into the synaptic cleft may lead to an increase in AMPAR-EPSCs. Alternatively, more release sites may become functional as the presynaptic calyx develops, leading to a selective increase in AMPAR-EPSCs without changing the total number of AMPARs on the MNTB neuron. In contrast, Taschenberger & von Gersdorff (2000) and Iwasaki & Takahashi (2001) showed that the size of AMPAR-EPSCs remains constant throughout the same developmental window in the rat calyx of the Held synapse. This discrepancy may reside in the different approaches used to identify synaptically connected MNTB neurons in slices, or alternatively in the species used. Recently, two separate reports from Takahashi's group showed that a genuine developmental difference in the size of AMPAR-EPSCs at the calyx of the Held–MNTB synapse indeed exists between rats and mice (Iwasaki & Takahashi, 2001; Futai *et al.* 2001). Our results are in good agreement with the mouse study (Futai *et al.* 2001).

Unlike previous studies showing a gradual decrease in NMDAR-EPSC amplitude at calyx-type synapses (Bellingham *et al.* 1998; Taschenberger & von Gersdorff, 2000), we have shown that there are relatively more NMDARs than AMPARs at P3/4 and that this ratio reverses after presynaptic terminals have made contact with their postsynaptic targets after P5/6 (Fig. 3). We observed an initial increase in both the synaptic NMDAR-EPSC- and NMDA-evoked whole-cell current prior to the onset of sensory inputs at P11/12 followed by a decrease in these currents. Most strikingly, NMDARs virtually disappear in mature MNTB neurons after P16 (Figs 2 and 3), raising the possibility that functional hearing downregulates synaptic NMDARs in an activity-dependent manner.

We have also observed acceleration in the decay kinetics of both NMDAR and AMPAR-EPSCs at this synapse. It is generally agreed that different subunit compositions underlie the gating kinetics of the NMDAR channel and hence developmental changes in the kinetics of NMDAR-EPSCs (Carmignoto & Vicini, 1992; Hestrin, 1992; Takahashi *et al.* 1996; Flint *et al.* 1997). For example, increased expression in NR2A has been associated with an accelerated time course of the NMDAR-EPSC (Takahashi *et al.* 1996; Flint *et al.* 1997; Tovar & Westbrook, 1999; Cathala *et al.* 2000). Our pharmacological analyses using subunit-specific reagents including ifenprodil, Zn^{2+} or TPEN only revealed very little change in the sensitivity of synaptic NMDARs to these drugs. Both Zn^{2+} and TPEN which target NMDARs containing NR2A subtypes produced less than 10 % change in NMDAR-EPSCs at any given developmental stage, while ifenprodil, which selectively blocks NMDARs containing NR2B subtypes, led to about 25 % inhibition. These subtle developmental changes lend little evidence to support the possibility of simple subunit switching from NR2B to NR2A, as shown for other central synapses (Takahashi *et al.* 1996; Flint *et al.* 1997; Tovar & Westbrook, 1999; Cathala *et al.* 2000). However, we cannot exclude the possibility that NMDARs may consist of three or more different subunits, which would have distinctive pharmacological phenotypes to these reagents. Nevertheless, we noted that the significant decrease in the decay time constant of NMDAR-EPSCs occurred at P11/12 (Fig. 4*D*), the same age at which we also observed an increase in Mg^{2+} block (Fig. 5*F*). This may be correlated with a reduction in NR2C and NR2D in synaptic NMDARs. Alternatively, profound morphological transformation of the calyx from spoon- to finger digit-like shapes within the first two postnatal weeks (Morest, 1968; Kuwabara *et al.* 1991) may directly influence the kinetics of NMDAR-EPSCs. Spoon-shape calyces may trap glutamate at release sites located in the central part of terminals, leading to rebinding of glutamate to NMDARs, which would slow the decay of NMDAR-EPSCs.

The decay kinetics of AMPAR-EPSCs can be influenced by channel gating, desensitization and the dynamics of glutamate in the synaptic cleft (e.g. release, clearance, etc.). Chuhma & Ohmori (1998) suggested that asynchrony of fusion events in immature synapses led to a longer decay time. Taschenberger & von Gersodorff (2000) and Iwasaki &Takahashi (2001) showed that there is a reduction in the

width of mEPSCs independent of asynchronous release. Although these conflicting results remain to be reconciled in future studies, subunit switching likely underlies accelerated decay of AMPAR-EPSCs at the calyx of the Held-MNTB synapse. Several reports have already shown that AMPARs containing GluR4 subunit may mediate fast synaptic transmission in rat and chick auditory synapses (Geiger *et al.* 1995; Otis *et al.* 1995; Zhou *et al.* 1995; Wang *et al.* 1998; Caicedo & Eybalin, 1999; Ravindranathan *et al.* 2000). Given that NMDARs play an indispensable role in developmental plasticity of immature synapses, we suggest that the transient presence of NMDARs prior to the onset of sensory inputs may provide sufficient Ca^{2+} influx for the recruitment, clustering and subunit switching of AMPARs in the postsynaptic density. NMDARs are, however, gradually removed to prevent Ca^{2+} overloading particularly during high-frequency transmission, as both the density of synaptic AMPARs and their Ca^{2+} permeability (e.g. GluR4) increase to a critical level sufficient for further refinement of synaptic properties and support of Ca^{2+}-dependent intracellular events. It remains to be resolved whether developmental reduction in NMDARs improves the fidelity of high-frequency transmission of spikes across this synapse (Taschenberger & von Gersodorff, 2000; Futai *et al.* 2001).

We have observed that there is an age-dependent reduction in the number of failures at the calyx of the Held–MNTB synapse during high-frequency transmission. These failures were shown to be due to presynaptic spike failures and independent of extracellular Ca^{2+} concentrations. It is conceivable that high-frequency firing may lead to K^+ accumulation in the extracellular space, which would lead to axon conduction failures. Alternatively, voltage-gated conductances are yet to be fully developed in immature calyces to enable high-frequency firing. The latter idea is supported by our observation that the spike width from immature terminals (e.g. P7, Fig. 6*F* and *G*) is broader than more mature calyces and therefore has a longer refractory period. We suggest that the narrowing spike width during development may increase the firing capacity of the calyx and also reduce synaptic depression by restricting the number of vesicles released in response to each action potential. Indeed, the extent of synaptic depression was strongly age-dependent, being most robust in immature synapses (e.g. P6–9 synapses in Figs 6–8). There are several elements that may contribute to such robust depression. First, the morphological structure (i.e. spoon-shaped calyx) at early postnatal stages of calyces may prevent glutamate from being rapidly removed and hence promote desensitization of synaptic AMPARs. Second, there is evidence that the size of the RRP of synaptic vesicles gradually increases as synapses progressively mature (Taschenberger & von Gersodorff, 2000; Iwasaki & Takahashi, 2001). The small size of RRP in young synapses is more prone to depletion when stimulated at a high rate. Finally, we have demonstrated that recovery from depression in immature synapses is substantially slower than more mature synapses (Fig. 8). These presynaptic changes in synaptic failures, depression and recovery, along with concurrent postsynaptic changes in the size and kinetics of glutamate receptors, ultimately lead to the maturation of high-fidelity synaptic transmission at the calyx of Held–MNTB synapses. Such transmission is of significant importance for the development of the phase-locking capacity in the mammalian auditory brain.

REFERENCES

Bellingham, M. C., Lim, R. & Walmsley, B. (1998). Developmental changes in EPSC quantal size and quantal content at a central glutamatergic synapse in rat. *Journal of Physiology* **511**, 861–869.

Bliss, T. V. P. & Collingridge, G. L. (1993). A synaptic model of memory: long-term potentiation in the hippocampus. *Nature* **361**, 31–39.

Caicedo, A. & Eybalin, M. (1999). Glutamate receptor phenotypes in the auditory brainstem and mid-brain of the developing rat. *European Journal of Neuroscience* **11**, 51–74.

Carmignoto, G. & Vicini, S. (1992). Activity-dependent decrease in NMDA receptor responses during development of the visual cortex. *Science* **258**, 1007–1011.

Cathala, L., Misra, C.& Cull-candy, S. (2000). Developmental profile of the changing properties of NMDA receptors at cerebellar mossy fiber-granule cell synapses. *Journal of Neuroscience* **20**, 5899–5905.

Chuhma, N. & Ohmori, H. (1998). Postnatal development of phase-locked high-fidelity synaptic transmission in the medial nucleus of the trapezoid body of the rat. *Journal of Neuroscience* **18**, 512–520.

Clements, J. D. (1996). Transmitter time course in the synaptic cleft: its role in central synaptic function. *Trends in Neurosciences* **19**, 163–171.

Crair, M. C. & Malenka, R. C. (1995). A critical period for long-term potentiation at thalamocortical synapses. *Nature* **375**, 325–328.

Cull-Candy, S., Brickley, S. & Farrant, M. (2001). NMDA receptor subunits: diversity, development and disease. *Current Opinion in Neurobiology* **11**, 327–335.

Flint, A. C., Maisch, U. S., Weishaupt, J. H., Kreigstein, A. R. & Monyer, H. (1997). NR2A subunit expression shortens NMDA receptor synaptic currents in developing neocortex. *Journal of Neuroscience* **17**, 2469–2476.

Forsythe, I. D. & Barnes-Davies, M. (1993). The binaural auditory pathway: excitatory amino acid receptors mediate dual time course excitatory postsynaptic currents in the rat medial nucleus of the trapezoid body. *Proceedings of the Royal Society* B **251**, 151–157.

Futai, K., Okada, M., Matsuyama, K. & Takahashi, T. (2001). High-fidelity transmission acquired via a developmental decrease in NMDA receptor expression at an auditory synapse. *Journal of Neuroscience* **21**, 3342–3349.

Geiger, J. R., Melcher, T., Koh, D. S., Sakmann, B., Seeburg, P. H., Jonas, P. & Monyer, H. (1995). Relative abundance of subunit mRNAs determines gating and Ca^{2+} permeability of AMPA receptors in principal neurons and interneurons in rat CNS. *Neuron* **15**, 193–204.

Hestrin, S. (1992). Developmental regulation of NMDA receptor-mediated synaptic currents at a central synapse. *Nature* **357**, 686–689.

Ishikawa, T. & Takahashi, T. (2001). Mechansims underlying presynaptic facilitatory effect of cyclothiazide at the calyx of Held in juvenile rats. *Journal of Physiology* **533**, 423–431.

Iwasaki, S., Takahashi, T. (2001). Developmental regulation of transmitter release at the calyx of Held in rat auditory brainstem. *Journal of Physiology* **534**, 861–871.

Izumi, Y. & Zorumski, C. F. (1995). Developmental changes in long-term potentiation in CA1 of rat hippocampal slices. *Synapse* **20**, 19–23.

Joshi, I. & Wang, L. Y. (2000). Postnatal development of synaptic properties in the mouse auditory brainstem. *Society for Neuroscience Abstracts* **30**, 1397 (524.5).

Kirkwood, A., Lee, H. K. & Bear, M. F. (1995). Co-regulation of long-term potentiation and experience-dependent synaptic plasticity in visual cortex by age and experience. *Nature* **375**, 328–331.

Kuwabara, N., DiCaprio, R. A. & Zook, J. M. (1991). Afferents to the medial nucleus of the trapezoid body and their collateral projections. *Journal of Comparative Neurology* **314**, 684–706.

McBain, C. J. & Mayer, M. L. (1994). N-methyl-D-aspartic acid receptor structure and function. *Physiological Reviews* **74**, 723–760.

Malenka, R. C. (1994). Synaptic plasticity in the hippocampus: LTP and LTD. *Cell* **78**, 535–538.

Morest, D. K. (1968). The growth of synaptic endings in the mammalian brain: a study of the calyces of the trapezoid body. *Zeitschrift für anatomie und Entwicklungsgeschichte1* **27**, 201–220.

Otis, T. S., Raman, I. M. & Trussell, L. O. (1995). AMPA receptors with high Ca^{2+} permeability mediate synaptic transmission in the avian auditory pathway. *Journal of Physiology* **482**, 309–315.

Paoletti, P., Ascher, P. & Neyton, J. (1997). High-affinity zinc inhibition of NMDA NR1-NR2A receptors. *Journal of Neuroscience* **17**, 5711–5725.

Patneau, D. K., Vyklicky, L. Jr. & Mayer, M. L. (1993). Hippocampal neurons exhibit cyclothiazide-sensitive rapidly desensitizing response to kainate. *Journal of Neuroscience* **13**, 3496–3509.

Ravindranathan, A., Donevan, S. D., Sugden, S. G., Grieg, A., Rao, M. S. & Parks, T. N. (2000). Contrasting molecular composition and channel properties of AMPA receptors on chick auditory and brainstem motor neurons. *Journal of Physiology* **523**, 667–684.

Stocca, G. & Vicini, S. (1998). Increased contribution of NR2A subunit to synaptic NMDA receptors in developing rat cortical neurons. *Journal of Physiology* **507**, 13–24.

Taschenberger, H. & Von Gersdorff, H. (2000). Fine-tuning an auditory synapse for speed and fidelity: Developmental changes in presynaptic waveform, EPSC kinetics, and synaptic plasticity. *Journal of Neuroscience* **20**, 9162–9173.

Takahashi, T., Feldmeyer, D., Suzuki, N., Onodera, K., Cull-candy, S. G., Sakimura, K. & Mishina, M. (1996). Functional correlation of NMDA receptor epsilon subunits expression with the properties of single-channel and synaptic currents in the developing cerebellum. *Journal of Neuroscience* **16**, 4376–4382.

Tovar, K. R. & Westbrook, G. L. (1999). The incorporation of NMDA receptors with a distinct subunit composition at nascent hippocampal synapses *in vitro*. *Journal of Neuroscience* **19**, 4180–4188.

Trussell, L. O. (1999). Synaptic mechanisms for coding timing in auditory neurons. *Annual Reviews in Physiology* **61**, 477–496.

Trussell, L. O., Zhang, S. & Raman, I. M. (1993). Desensitization of AMPA receptors upon multiquantal neurotransmitter release. *Neuron* **10**, 1185–1196.

von Gersdorff, H., Schneggenburger, R., Weis, S. & Neher, E. (1997). Presynaptic depression at a calyx synapse: the small contribution of metabotropic glutamate receptors. *Journal of Neuroscience* **17**, 8137–8146.

Wang, L. Y. (2000). The dynamic range for gain control of NMDA receptor-mediated synaptic transmission at a single synapse. *Journal of Neuroscience* **20**, 1–5.

Wang, L. Y. & Kaczmarek, L. K. (1998). High-frequency firing helps replenish the readily releasable pool of synaptic vesicles. *Nature* **394**, 384–388.

Wang, Y. X., Wenthold, R. J., Ottersen, O. P. & Petralia, R. S. (1998). Endbulb synapses in the anteroventral cochlear nucleus express a specific subset of AMPA-type glutamate receptor subunits. *Journal of Neuroscience* **18**, 1148–1160.

Williams, K. (1993). Ifenprodil discriminates subtypes of the N-methyl-D-aspartate receptor: selectivity and mechanisms at recombinant heteromeric receptors. *Molecular Pharmacology* **44**, 851–859.

Xiong, Z., Pelkey, K. A., Lu, W. Y., Lu, Y. M., Roder, J. C., MacDonald, J. F. & Salter, M. W. (1999). Src potentiation of NMDA receptors in hippocampal and spinal neurons is not mediated by reducing zinc inhibition. *Journal of Neuroscience* **19**, 1–6.

Yamada, K. A. & Rothman, S. M. (1992). Diazoxide blocks glutamate desensitization and prolongs excitatory postsynaptic currents in rat hippocampal neurons. *Journal of Physiology* **458**, 409–423.

Zhou, N., Taylor, D. A. & Parks, T. N. (1995). Cobalt-permeable non-NMDA receptors in developing chick brainstem auditory nuclei. *NeuroReport* **6**, 2273–2276.

Zucker, R. S. (1989). Short-term synaptic plasticity. *Annual Reviews in Neuroscience* **12**, 13–31.

Acknowledgements

This work was supported by an individual operating grant, 'The Synapse' group grant from Canadian Institutes of Health Research (CIHR), and by a start-up fund from the Hospital for Sick Children (HSC) Research Institute. I. J. is a recipient of the Ontario Graduate Scholarship (OGS) and the HSC Research and Training Center Studentship. L. Y. W. is a CIHR New Investigator. We would like to thank Shahira Shokralla, Tina Epps and Zoltan Nagy for assistance and discussion.